Non Boltzmann Modeling of Sodium Guidestar Returns and Implications for Guidestar Linewidth

Shawn Hackett,[a]* Robert Johnson,[a] Jack Drummond[a]
[a]Air Force Research Lab, Directed Energy Directorate, Starfire Optical Range (SOR), Kirtland AFB, NM 87117

Abstract. To date, modeling of sodium guidestar mesospheric excitation has assumed that the distribution within the sodium ground states (F = 1 or F = 2) and the distribution between the two ground states was well modeled by a Maxwell-Boltzmann distribution. Recent experimental evidence from Starfire Optical Range and the modeling results of Bhamre et al., show that the Maxwell-Boltzmann distribution is not a good approximation for the velocity distribution within ground states after optical excitation by a narrowband laser (linewidth < 1 MHz). A model is presented to account for the non-Boltzmann effects on the velocity groups of the Doppler profile of the mesospheric sodium atoms. The model is shown to agree fairly well with data provided from the 3.5m telescope and narrowband laser guidestar at Starfire Optical Range. These results challenge the efficacy of reducing the linewidth of sodium laser guidestars below 1 MHz.

Keywords: guidestar modeling, sodium guidestar, Starfire Optical Range, fiber laser guidestar

***First Author, E-mail: shawn.hackett.1@us.af.mil

1 Introduction

A sodium guidestar is an artificial star used to create a cooperative source for coherent imaging of small, dim objects in space.

1.1 Excitation of Mesospheric Sodium

Narrowband excitation (source bandwidth < 10 MHz) of sodium atoms with circularly polarized light allows for continual pumping of the idealized F=2 to F=3 transition and mitigates many effects of saturation [2]. Figure 1.1 shows the sodium hyperfine structure diagram for reference. Figure 1.2 shows the result of Kibblewhite on broad vs. narrowband pumping. Broadband pumping was shown to quickly saturate the sodium concentration in the mesosphere [5]. Therefore, sodium guidestar development focused on narrowband sources for excitation of the sodium layer. Atoms which have velocities not tangential to the guidestar's beam or which are in the F=1 ground state cannot interact with guidestar and will not produce return. This entire development relies on repopulation of the mesospheric sodium Doppler profile area which can interact with guidestar by two effects [4]. Oxygen spin exchange is the process which repopulates atoms from the F=1 ground state to the F=2 ground state. Velocity changing collisions result in energy exchanges between sodium atoms. These collisions cause the shifting of sodium

atoms to different areas within the Doppler profile. Different areas of the Doppler profile obviously have different velocities with respect to the laser's radiation field. The coefficients associated with each of these effects are known as v_S and v_{cc} respectively[5].

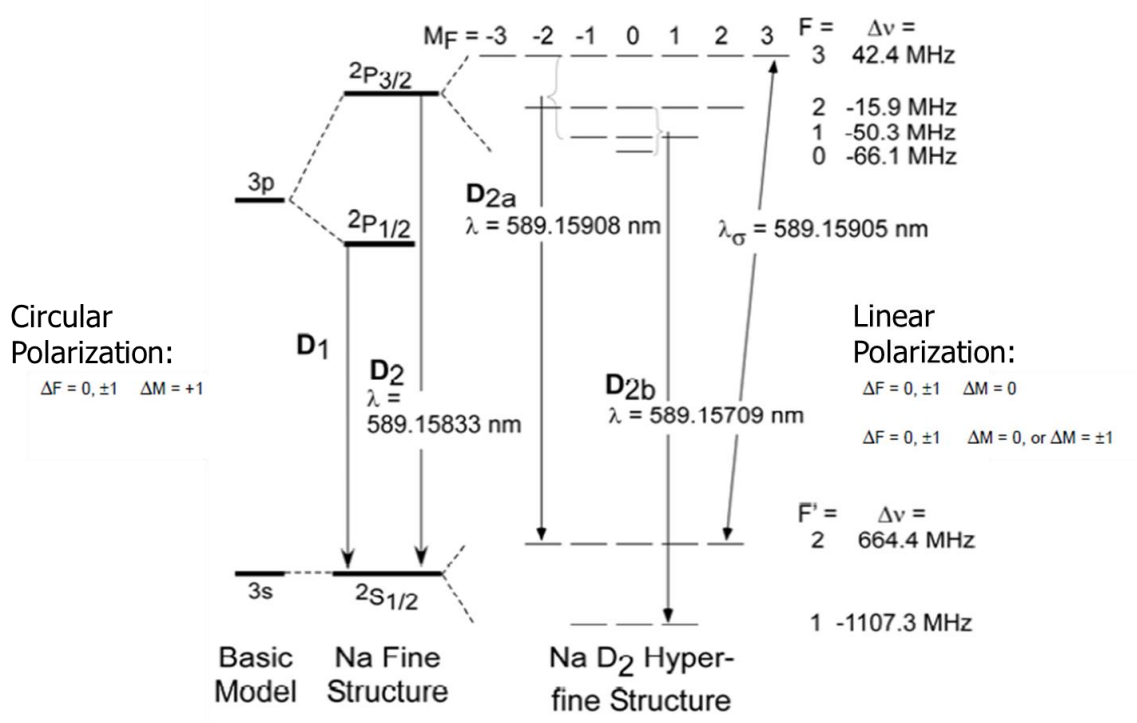

Figure 1.1: Sodium Hyperfine Structure Diagram [2]

1.2 Sodium Guidestar Repumping

Rather than relying solely on the effect of oxygen spin exchange with sodium to repopulate the F=2 state (D2a) from the F=1 state (D2b), one could actively pump D2a and D2b simultaneously to ensure that excited D2b atoms would have a chance to decay to F=2 rather than F=1. This occurs with even likelihood because of degeneracy. Such a scheme was first implemented at SOR by [2] as a proof of concept. The authors were able to increase the power output of a narrowband guidestar (MHz) with a narrowband repump by 1.6 times without good multi-beam alignment [2]. To idealize the pumping and repumping schemes a narrowband D2a source pump source (10 MHz) and a broadband D2b repump (1 GHz) could be combined to deliver a pump source which avoids D2a saturation and a repump source which saturates D2b completely and quickly.

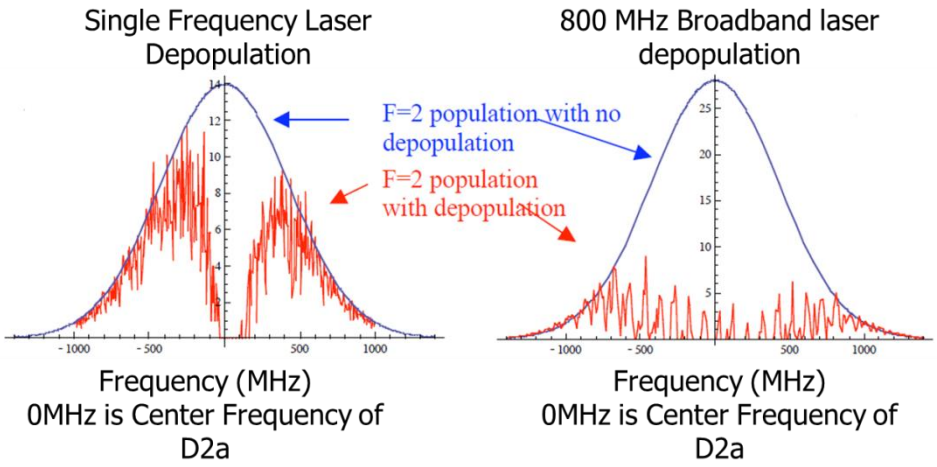

Figure 1.2: Narrowband vs. Broadband Pumping Saturation of D2a (F = 2 State) [5].

1.3 Sodium Guidestar Modelling

Previous sodium guidestar modelling comes in one of two types: a rate equation model such as [5] or Bloch equation models such as that of [4]. [4] provides an extensive listing of all previous sodium guidestar models, their strengths and weaknesses, and their design parameters. [4] also provides a detailed description of the setup of a freeware Mathematica guidestar model developed by Rochester Scientific and European Southern Observatory (ESO). This model is found to have very good agreement with experimental results and is highly adaptable and useful. For the purpose of this paper, all modelling is restricted to the use of a modified version of the Mathematica code provided at [6] whose input parameters and methodology can be found at [4].

2 Sodium Guidestar Model

This section describes the setup of sodium guidestar model used to predict and validate the performance of the sodium guidestar at SOR.

2.1 Model Setup

As stated above, the model used for this development is Mathematica Freeware created by Holzloehner and Rochester available at [6]. The model provides a complete Bloch equation development of the mesospheric sodium interaction with an input laser beam and the earth's magnetic field. The canonical Bloch equation from [4] is:

$$\frac{d\rho}{dt} = i\hbar[H,\rho] + \Lambda(\rho) + \beta \qquad (2.1)$$

$$H = H_0 + H_E + H_B \tag{2.2}$$

where ρ is the density of a given velocity class within a hyperfine state of the sodium atom. *H* is the total Hamiltonian (unperturbed energy, electric dipole interaction and magnetic dipole interaction summed). Λ(ρ) governs density dependent terms not in *H* (spontaneous decay, collisional spin relaxation, changes of atomic velocity due to collisions and emission induced recoil, and the movement of atoms into and out of the laser radiation field due to the movement of the atoms and of the laser beam. β describes terms not dependent on ρ such as repopulation of atomic velocity class and sublevels due to movement of atoms via the mesospheric wind. A more complete description is given in [4]. Equation 2.1 can be re-written as:

$$\frac{d\rho}{dt} = A\rho + b \tag{2.3}$$

where *A* is a matrix and *b* is vector that are independent of ρ. Equations such as Eq. 2.3 are then setup for separate velocity classes. To fully model all possible hyperfine transitions, vectors *b* and ρ must have 576 elements per velocity class. The model then uses a methodology to determine the ideal number of velocity classes. Typically, the linear equation system of Eq 2.3 has dimension 32,500 – 65,000 [4].

2.2 Input Parameters

A host of possible input parameters are listed in [4] though for this development only those of Table 2.1 were modified. This development focuses on the variation of the first four parameters (denoted laser parameters) to find their ideal values to enhance laser guidestar design and usage. The other parameters (denoted scenario parameters) are determined by either the sodium mesospheric physics, the atmospheric conditions, or the launch telescope being utilized and are not generally easily variable. Therefore, these parameters were only varied based on measured conditions to ensure agreement between modelling and observed data.

After setting up a scenario based on these input parameters, the model then determines a return photon flux, Φ (ph/s/m^2) at the top of the observing telescope, or the model can provide return flux per solid angle per intensity Ψ (ph/s/sr/(W/m^2) in the mesosphere. Φ may be thought of as a figure of merit for an entire guidestar system and Ψ

Table 2.1: Input Parameters varied in modelling effort

Parameter Name	Symbol	Typical Values
	Laser Parameters	
Launched Laser Power	P	*1 – 100 W*
Polarization Ellipticity Angle	χ	*0 – π/4*
Laser FWHM Linewidth	Δf	*0 – 2 GHz*
Repumping Power Fraction	q	*0 – 0.20*
	Scenario Parameters	
Zenith Angle	ζ	*0-60°*
Launch Telescope Altitude	H_{tele}	*1850 m*
Launch Telescope Aperture	D	*23 cm*
Launch Telescope Beam Radius	w	*9 cm*
Launched Beam RMS Wavefront Error	WFE	*100 nm*
Polar Angle of *B*	θ	*0 – π*
Azimuth Angle of *B*	φ	*0 – π*
Outer Turbulence scale	L_0	*10-50 m*
Geomagnetic Field Strength	B	*0.48 G*
One way transmission at Zenith	T_a	*0.75-0.9*
Mesospheric Temperature	T_{NA}	*180 – 200 K*
Sodium Centroid Altitude	H_{NA}	*90 – 96 km*
Sodium Column Density	CAN	*1.8 – 10.0 x 10^{13} m^{-2}*
Weighted velocity changing collision rate	γ_{Vcc}	*1 / (35 μs) See Equation 2.6*
Weighted Spin Exchange Rate	γ_S	*1 / (490 μs) See Equation 2.7*
Beam atom exchange rate	γ_{ex}	*1/(6.0 ms)*

may be thought of as a figure of merit for the guidestar's ability to excite mesospheric sodium atoms. Hence, Φ is used to compare total ability of a guidestar system to provide a bright cooperative beacon for adaptive optics.Ψ is a parameter to compare overall guidestar efficiency in different scenarios and between different guidestars. This development will focus mainly on Φ as a figure of performance for simplicity, though both Φ and Ψ are important.

2.3 Non-Boltzmann Parameters

Most of the Λ(ρ) terms given in Section 2.1 and Section 2.2 are well understood and modelled and have no reason to be changed (radiation pressure, recoil, Larmor precession). Previous modelling assumed many parameters obeyed a Maxwell-Boltzmann distribution. Specifically, the parameters dealing with the change of distribution of atoms within velocity classes, the collisional repopulation between velocity classes, and the collisional repopulation between each ground state (F = 2 and F = 1) were modelled to obey a Maxwell-Boltzmann distribution as part of Λ(ρ). Several processes, such as spin exchange between oxygen and sodium, were modelled by another method and a more complete treatment is shown at [4]. This development is not a complete description of the behavior of atoms within each velocity class especially in the presence of a laser whose linewidth is fairly narrow (> 1MHz) as shown

by [1]. The author found that optical spectral hole burning by a very narrowband source (> 1MHz) led to non-Maxwell-Boltzmann behavior in velocity class repopulation and collisions of sodium atoms within each ground state and in-between each ground state [1]. Therefore, this development was used to modify rate coefficients in the model of [6]:

$$\gamma_{vcc} = 1/v_{cc} \quad (2.4)$$

$$\gamma_S = 1/v_S \quad (2.5)$$

$$v'_{cc} = v_{cc}(1 + Log[1 + \frac{M_{cc}}{\Delta f}]^2) \quad (2.6)$$

$$v'_S = v_S(1 + Log[1 + \frac{M_O}{\Delta f}]^2) \quad (2.7)$$

The new collisional rate coefficients in Eqs 2.6 and 2.7 were not determined physically, but represent a perturbation of original rate coefficient where M_{cc} and M_O represent the degree to which modifying the laser linewidth should affect a given rate coefficient. Good agreement with observed results was found when M_{cc} = 1MHz and M_O = 50kHz. Hence, the overall v_{cc} rate needs to be modified for more accuracy (a feature which can already be implemented in the Rochester/Holzloehner model) as laser linewidths below 1MHz are commonly possible for Sum Frequency Generation (SFG) guidestars; however, the current model for v_S is probably sufficient because guidestar linewidths below 50kHz are much less common. Further, the ratio of the effect on the output return flux from modifying v_s compared to v_{cc} by an equal percentage is 1/10. An equal change in v_{cc} yields a 10x greater effect in output versus an equal percentage change in v_S.

3 Experimental Setup

Guidestar returns were collected at the Starfire Optical Range (SOR) utilizing the SOR's 3.5m primary telescope and several additional platforms to launch laser guidestar sources. One source was a narrowband (~500 kHz) SFG guidestar, and one source was a new Toptica Sodium Star 20/2 with repumping and broader linewidth (~5MHz).

3.1 Launch and Receive Apertures and Typical Conditions at SOR

All guidestar return presented data was received via the 3.5m telescope at SOR. The SFG guidestar was launched by a 23 cm aperture, and the Toptica sodium star was launched with a 30 cm aperture. A picture of each guidestar is provided in Figure 3.1. One guidestar is observed on axis, and the other is observed slightly off-axis and thus appears as an elongated spot in the mesosphere 5-8 km in extent in the direction of propagation of the laser beam.

3.2 Typical Conditions at SOR

All other characteristics utilized were varied as shown in Table 2.1 to match scenario conditions: atmospherics, launched laser characteristics, telescopic configurations, and mesospheric sodium conditions. A map of return flux at SOR based on the variability of the magnetic field, from Drummond, is shown in Figure 3.2 for reference [3].

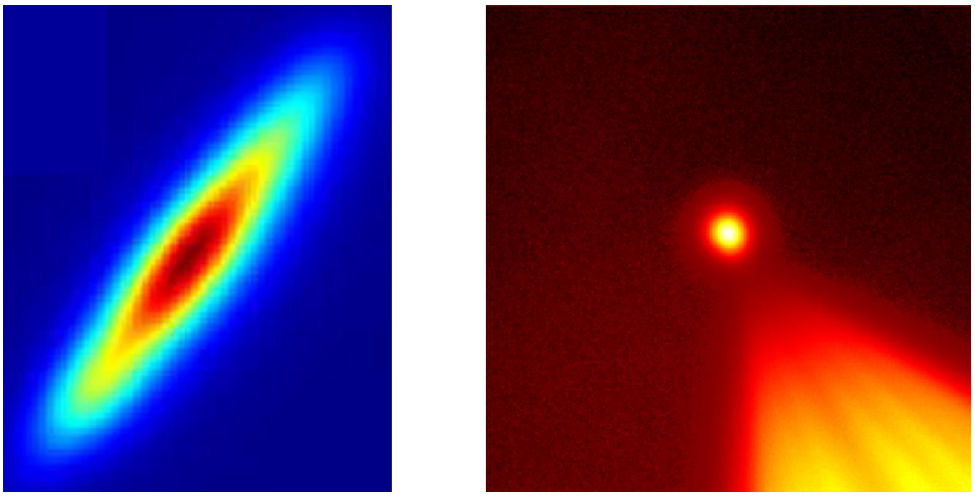

Figure 3.1: Toptica Sodium Star 20/2 (Left) and SFG Guidestar (Right) observed at SOR. The elongated spot on the left is due to off-axis observation of the guidestar. The large triangular region in the right image is due to Rayleigh scattering.

4 Experimental Results

The SFG guidestar and the Sodium Star 20/2 were compared for performance with varying powers. The SFG guidestar was found to offer similar performance at >40 W without repumping to the Sodium Star 20/2 at 15.4W with repumping. Figure 4.1 shows a strong degree of saturation as each incremental increase in power yields a lesser increase in return flux. Figures 4.2 and 4.3 show that saturation is not as strong or not present at all when circularly polarized light and/or repumping are utilized with a broader band guidestar. Figure 4.3 shows the variation in guidestar performance at the beginning and end of the same night (8 hours separation) due to the change in sodium concentration. The estimated seasonal average for guidestar performance is shown for comparison.

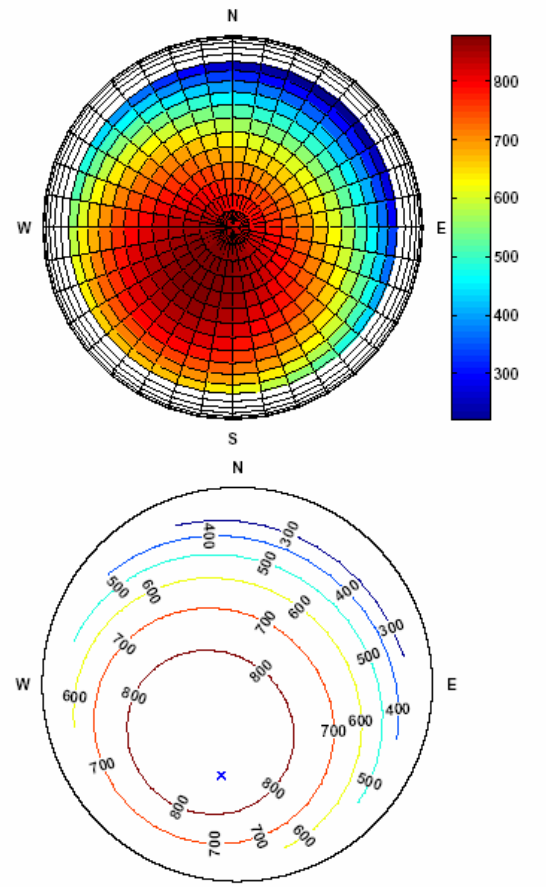

Figure 3.2: Contour Plots of Return Flux at SOR for different magnetic field azimuthal and polar angles. [3]

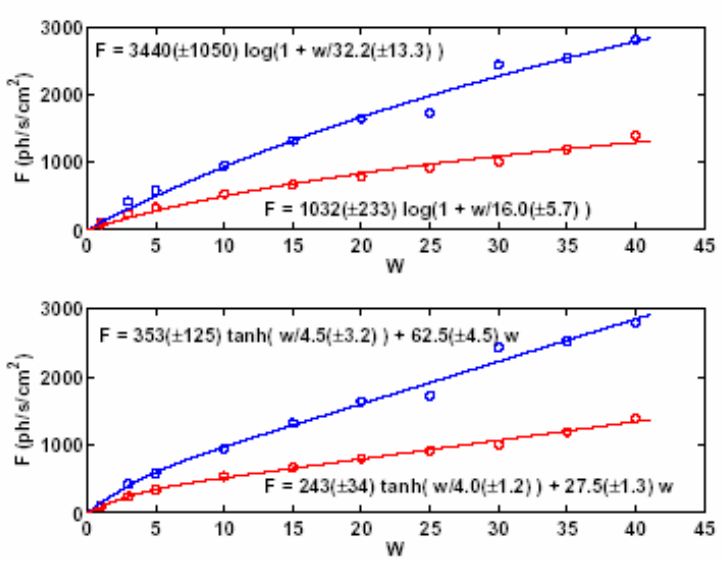

Figure 4.1: December 22, 2005 SFG guidestar performance for variable powers and pointing direction. The blue curves represent circular laser radiation performance and the red curves linear [3]

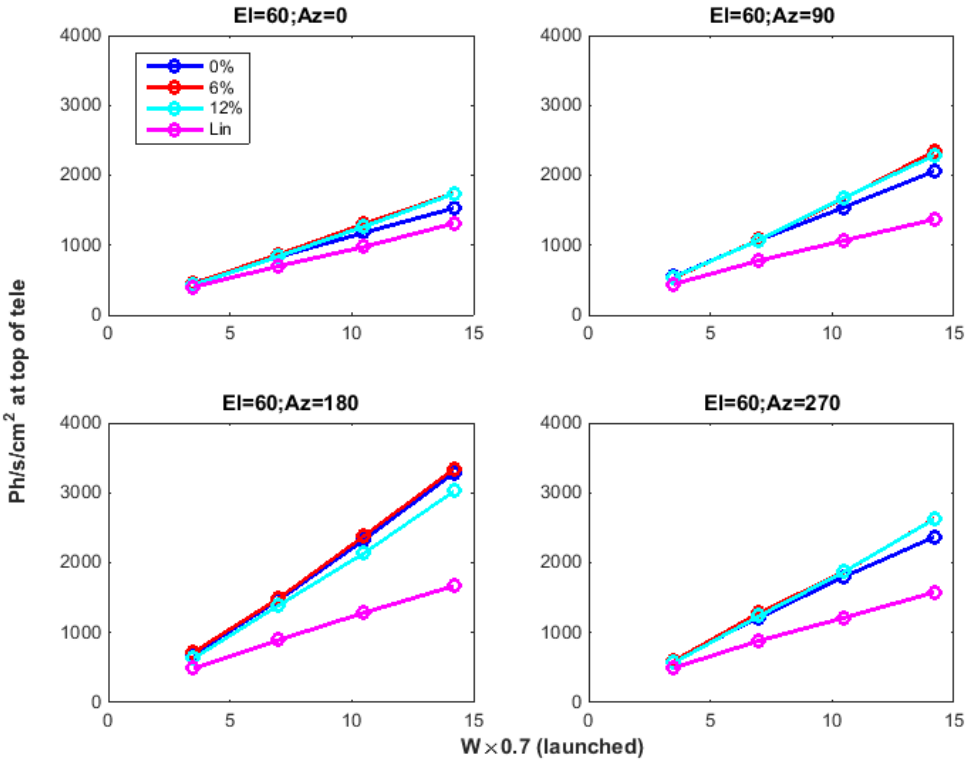

Figure 4.2: Nov 2, 2015 Performance of Sodium Star 20/2 for variable powers and pointing direction. The different curves represent different repumping ratios for circularly polarized laser radiation and linearly polarized laser radiation.

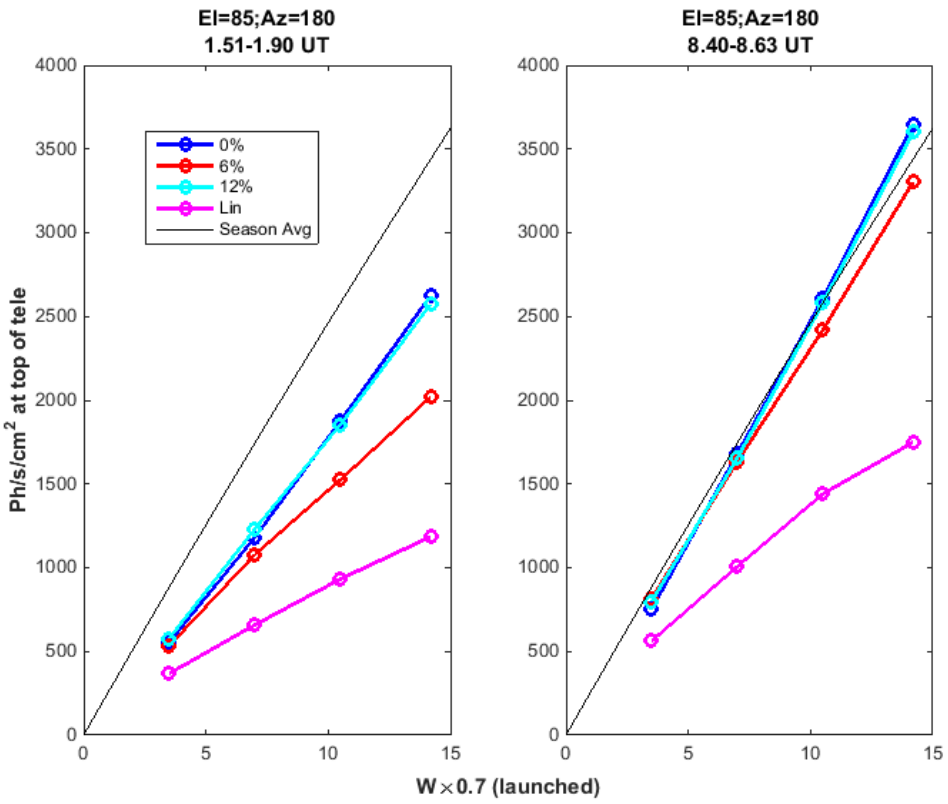

Figure 4.3: Nov 2, 2015 Performance of Sodium Star 20/2 for variable powers at different times of night.

5 Modelling Results and Analysis

Using the model, of Section 2, the parameters in Table 2.1, and the results of Section 4 yielded Figures 5.1, 5.2, and 5.3. Figure 5.1 shows the effect of varying bandwidth and total launched power without repumping while all other variables remain constant. Figure 5.2 shows the effects of varying bandwidth of both the D2a primary source and D2b repumping source while all other parameters remain constant. Figure 5.3 shows the varying effect of repumping in the case of different total launched laser powers and different primary (D2a) and repump (D2b) laser bandwidths, though the D2a and D2b laser source were modeled to have the same bandwidth.

5.1 Analysis of Modelling Results

Based on the modelled results from Figure 5.1, the ideal bandwidth for guidestar laser with only sodium D2a excitation is around 10 MHz which is very close to the sodium vacuum linewidth [7]. As discussed above, the model attempts to account for the effects of narrow frequency excitation as discussed in Section 2.3, and Figure 5.1 shows a very strong effect for lasers with linewidths narrower than *500 kHz*, as shown experimentally in Figures 4.1 and

4.2. Figure 4.2 shows that even modest repumping (6%) is very helpful and becomes more imperative as total launched power increases as shown in Figure 5.2 and Figure 5.3. Figure 5.3 further shows the effects of varying repumping ratios and the co-variant effects of bandwidth and total launched power. In Figure 5.3 both D2a and D2b bandwidth are equal.

5.2 Conclusions Based on Modeling

From Figure 5.1, the ideal bandwidth increases with increasing power. At powers below *25 W*, *5 MHz* is the ideal linewidth, but at powers above *25 W*, *10MHz* becomes more ideal. Figure 5.2 also shows that increasing the bandwidth of the D2b repumping while maintaining the bandwidth of the D2a primary source provides an increase in total return for powers above *35W*. Based upon the results of Figure 5.2, narrowband D2b repumping provides an increase in return flux of *2-3x* while broadband D2b repumping provides an increase in return flux of *2-4x* at launched powers between *20-60W*. Figure 5.3 shows even 1% repumping enhances return flux; however, the behavior of the effect of repumping seems to be independent of total launched laser power with powers greater than 50W. The only effect influencing the ideal choice of repump ratio in these cases seems to be the laser bandwidth. As stated above the ideal bandwidth is dependent upon total launched power. Hence, repump ratio, launched laser power, and ideal bandwidth must be co-optimized to find the ideal guidestar setup for optimal return flux. Idealized repumping was found to be between 7.5% (5 W) and 22% (200 W). SOR is currently using the results of this modelling effort to influence SOR's future guidestar designs.

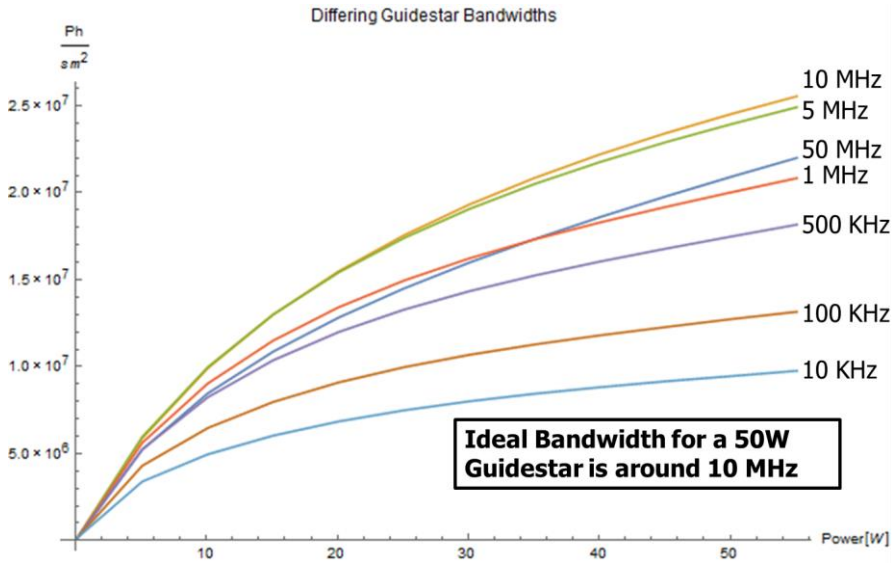

Figure 5.1: Modelled performance for different guidestar bandwidth with all other parameters constant

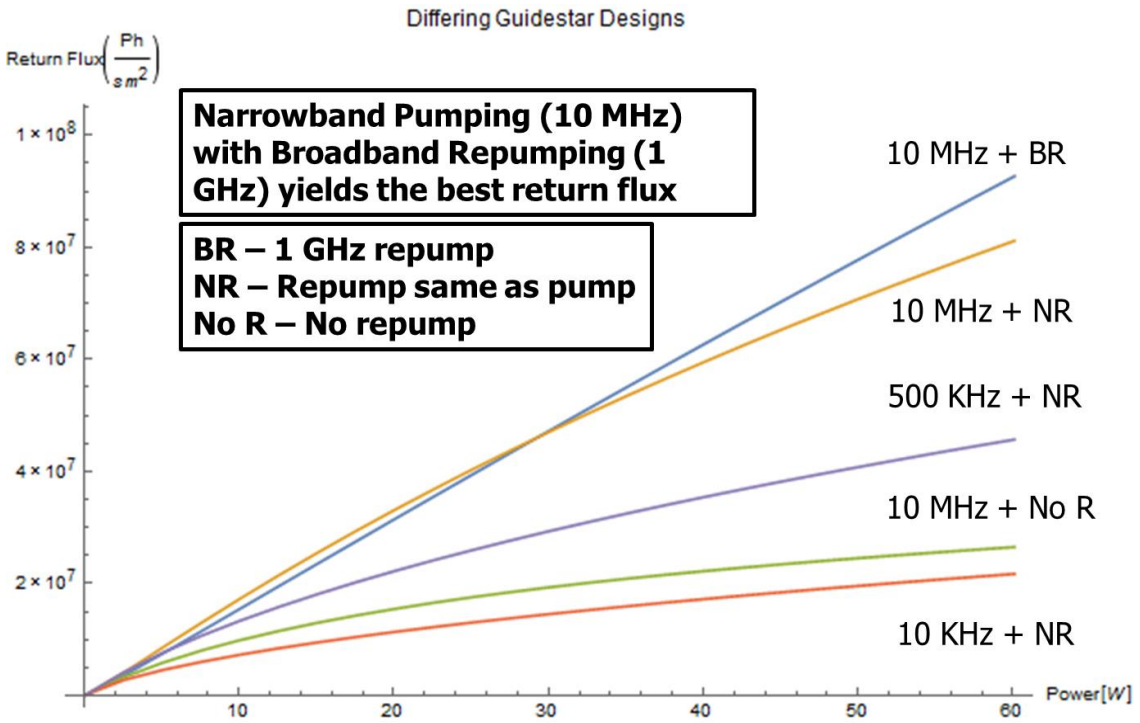

Figure 5.2: Modelled performance for different guidestar D2a and D2b bandwidths with a repumping ratio of 15% (except where noted) with all other parameters constant.

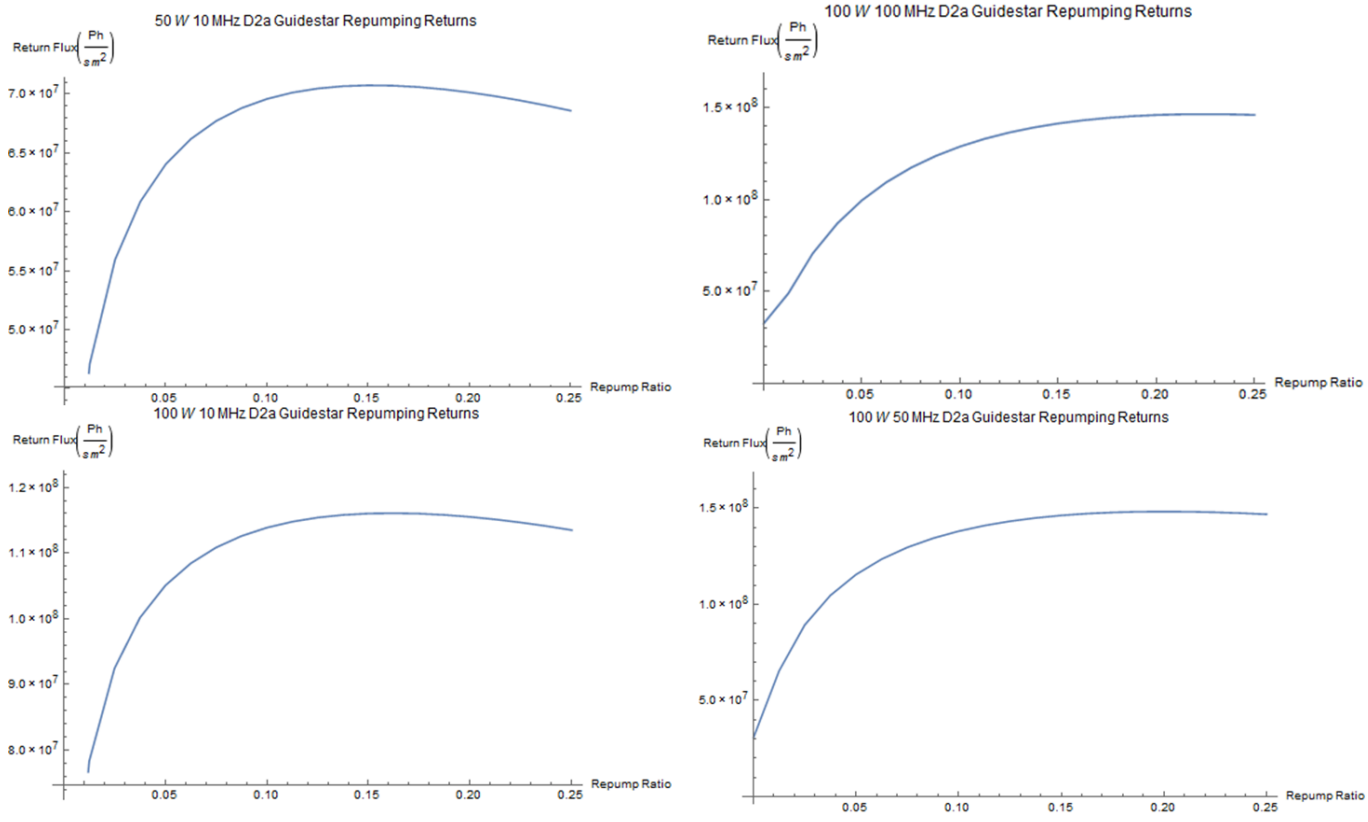

Figure 5.3: Modelled performance for different repump ratios varying total launched power and D2a/D2b bandwidth with all other parameters constant.

References

1. Bhamre et al. “Collision kernels from velocity selective optical pumping with magnetic depolarization” Physical Review A 87 Apr (2013).
2. Denman, C., SOR internal communication, May (2006).
3. Drummond, J. et al., “Sodium Guidestar Radiometry Results from the SOR’s 50W FASOR” AMOS Conference Proceedings Sept (2006).
4. Holzloehner et al. “Optimization of cw sodium laser guide star efficiency” Astronomy & Astrophysics Oct (2009).
5. Kibblewhite, E. “The Physics of Sodium Laser Guidestars: Predicting and Enhancing the Photon Return” Jan (2009)
6. Rochester, S. “Atomic Density Matrix” http://rochesterscientific.com/ADM/, Aug (2015).
7. Ungar, P. J., Weiss, D. S., Riis, E., and Chu, S., “Optical molasses and multilevel atoms: theory,” J. Opt. Soc.Am. B. Vol. 6, No. 11, Nov (1989).